DOI 10.4430/bgo00410

Seismic demand assessment of structural glass systems based on simplified methods

S. Mattei and C. Bedon

University of Trieste, Department of Engineering and Architecture, Trieste, Italy

(Received: 8 April 2022; accepted: 7 November 2022; published online: 30 November 2022)

ABSTRACT Although glass is frequently used as a structural component for buildings and infrastructure (façades, floors, walkways, etc.), also in combination with other construction materials, the regulatory framework as a guideline for the design stage is still limited. Many studies, in this regard, have focused on the definition of glass material characteristics and structural behaviour under various design loads, especially unfavourable conditions. The aim of the present work is to verify the reliability of available simplified methods for glass systems during earthquakes, based on the definition of seismic response spectra, and to help define a robust method to verify seismic capacity through the use of specific fragility curves. Two case-study systems made of glass are examined. Seismic hazards of particular sites are considered for each limit state and soil type, and results of simplified calculations for rapid assessment of seismic demand are compared with more refined but computationally expensive finite element non-linear dynamic analyses.

Key words: structural glass, earthquakes, seismic design, seismic demand assessment, fragility curves, dynamic non-linear analyses.

1. Introduction

Glass is a fairly popular material for many types of structural applications, such as commercial, civil and industrial buildings, both playing a primary load-bearing role and a secondary role for glazing elements without structural functions. A constructional component can be defined as 'structural' when it is designed to withstand loads due to internal or external actions for the duration of its life. Different design demands are required for 'secondary structural' or 'non-structural' components (Bedon *et al*., 2019a). Although glass has intrinsic limits because of its brittleness in tension, low fire resistance and the possibility of producing fragments that could damage human health during exceptional events, in recent years it has shown promising applications for safe applications as a structural component (Haldimann, 2006; Haldimann *et al.*, 2008), in the form of beams, columns, façades, walkways, or bridges (Niedermaier, 2003; Netusil and Eliasova, 2012; Shelby, 2020).

In general terms, it is recognised that the structural design of glass systems with respect to eventual accidents and extreme events is rather challenging (Bedon *et al.*, 2018). Several authors have focused on the capacity of glass structures subjected to wind loads (Behr *et al.*, 1996; Gavanski, 2010), hurricane loads (Beason *et al.*, 1984; Venkata, 2004), blast events (Larcher *et al.*, 2016), and seismic loads (Behr, 1998; Brueggeman *et al.*, 2000; Dean *et al.*, 2006; Memari *et al.*, 2011; Puga *et al.*, 2015; Huang *et al.*, 2017), in order to provide engineering knowledge to support the design.

Especially for seismic engineering purposes, experimental tests on structural glass systems and mock-up prototypes are of primary importance for seismic capacity assessment, but can be rather expensive and complex. Careful attention should be given to single components (i.e. glass panels, details), but also to the global performance optimisation, including connection details. In this regard, simplified analytical methods can be computationally expensive and their accuracy could be compromised. In the same way, several numerical investigations have been performed to evaluate experimental findings, by taking advantage of different modelling approaches and computational environments, such as SAP200 (Aiello *et al.*, 2018), ANSYS (Memari *et al.*, 2011) or ABAQUS (Mattei and Bedon, 2021; Tahmasebinia *et al.*, 2021). Regarding glass systems as a part of complex three-dimensional buildings under seismic events, the advanced design of special restraints can also facilitate the implementation of dissipative systems for mitigation purposes, and promising applications have been theoretically observed for both stand-alone seismic events (Bedon and Amadio, 2019) or even multi-hazard scenarios (Bedon and Amadio, 2018).

Currently, the regulatory framework for seismic design and verification of glass elements is poor because technical recommendations (if any) are limited to a few particular configurations (i.e. setup, boundaries), which do not fully cover the majority of possible applications of practical interest for glass components in buildings. In general, moreover, both European and even non-European seismic design codes for buildings provide a set of limits for strength and displacement parameters, but do not suggest constructional details to preserve a sufficient load-bearing capacity and displacement accommodation of seismic demand. At the national level, as an extension of seismic provisions by the Italian NTC (2018) design code of practice, specific guidelines for structural glass design can be taken from the CNR-DT210 (2013) technical instructions issued by the National Research Council.

In this paper, an existing simplified calculation approach for preliminary seismic demand assessment of glass elements is used and evaluated for the analysis of two different case-study systems made of glass (CS#1 and CS#2, in the following). The simplified method, as shown, is applied according to Annex § 4.11 of CNR-DT210 (2013) guideline, and is based on response spectra estimation of displacement demand. In order to assess the potential and limits of this pre-sizing simplified procedure for different construction solutions made of glass, a quantitative comparison of seismic drift demand for CS#1 and CS#2 systems is elaborated with the contribution of advanced Finite Element (FE) numerical analyses carried out in ABAQUS/Explicit software (Simulia, 2022). The scatter between advanced FE numerical results and simplified analytical estimates is hence discussed, based also on various international standards for structural design of buildings and curtain walls [NTC (2018), EC8 (1998), ASCE7-10 (2013), and JASS14 (1996)].

2. General design recommendations and seismic design criteria for glass systems

Irrespective of the mechanical characteristics or specifications for each type of traditional building material (i.e. concrete, steel, masonry, wood), the design philosophy of existing seismic codes for constructions is based on damage limitation requirements. As such, inter-story drift provisions are usually given for Serviceability and Ultimate Limit States (LSs) associated with the occurrence of different damage levels. In this framework, elements and assemblies made of glass are generally considered as ‘secondary’ components, thus required to accommodate the deformations of the primary structures, while still being able to withstand vertical loads

(Bedon *et al.*, 2019a). Furthermore, their stiffness and strength to horizontal actions are disregarded in the global seismic analysis of primary structures, and local seismic analyses are only required.

For vertical glass elements, like curtain walls and façade components, horizontal displacements during seismic events are typically associated with the majority of expected damage. According to some full-scale experimental pieces of evidence (Sivanerupan *et al.*, 2014; Caterino *et al.*, 2017), it is assumed that glass fall-out corresponds to collapse for curtain walls. In order to limit the consequences of possible glass shattering, special attention should, thus, be given to the basic principles of structural glass design, namely safety, robustness, and redundancy. In particular, structural reliability as a probabilistic measure of structural safety depends on the importance of the building and the potential economic, social or life-loss consequences of the damage. As such, three consequences classes (CCs) are defined on the basis of UNI EN1990 (CC1 to CC3), to which the CNR-DT210 (2013) guideline adds the CC0 class for typically non-structural elements (and limited losses). Such kind of indication determines the required checks to carry out, by taking into account, for glass cracking, the context in which the glass element is present, the hazard in the event of failure, and the existence of countermeasures.

According to conventional seismic design codes for traditional buildings, as well as structural glass systems, the design seismic action depends on the importance class (C_u), the design life (V_R) and the performance levels (namely OLS = Operational, DLS = Damage, SLS = Safeguard of human life, and CLS = Collapse LSs). Moreover, designers must refer to particular drift values associated with the required performance levels against the input seismic action. Its representation can take several forms. The more accurate method involves the use of earthquake records, which are representative of time-histories of ground accelerations of a point along three main directions. Unfortunately, this representation is as rich in information as it is specific for a single event. For safety checks, according to § 7.3.5 of NTC (2018), it is, thus, required that the analysis of a given structure would be subjected to a family of seven acceleration stories for each direction of motion, with characteristics corresponding to those of possible future earthquakes. Consequently, in order to generalise and streamline structural calculations, the most frequently used tool in seismic engineering applications takes the form of response spectrum. According to some assumptions and simplifications, a simplified approach is hence proposed in Annex § 4.11 of CNR-DT210 (2013) and extensively addressed in the present study.

3. Considerations on available methods for seismic demand assessment

As it is known, seismic drift demand on buildings can be investigated in many ways, using elastic or inelastic approaches, with static or dynamic analyses. According to Section 2, the seismic stress calculation involves several aspects with major implications of probability theory, given the randomness of the variables involved, starting from the effective seismic intensity (on the loading side) to the actual properties of constituent materials (on the structural side). In contrast to other types of loads such as gravitational loads, seismic events are extreme loads and their intensity can be estimated only with a certain level of approximation, thus, referring to a probability of occurrence function of the time-parameter. The available mathematical models, based on limited observations of past events, allow acquiring a restricted knowledge of when a seismic event will occur, but also to observe that the longer the period considered (return period, T_R) and the greater the probability of having an earthquake of a certain intensity.

3.1. Italian code provisions and main assumptions of seismic demand assessment methods

In design practice, the seismic action is synthetically represented by a response spectrum in acceleration, or displacement. This tool represents the maximum response of an elastic Single Degree of Freedom (SDOF) system having variable period *T* and assigned damping x. The primary feature of design spectrum is the 'uniform hazard' characteristic, which means that whatever the considered *T*, the corresponding point of spectrum always has the same probability of occurrence. Hence, after the definition of basic parameters (such as site location, geological and morphological category of soil, and importance class of construction), T_R is given by:

$$T_R = \frac{V_R}{ln\left(1 - P_{VR}\right)} = \frac{C_U V_N}{ln\left(1 - P_{VR}\right)} \tag{1}$$

and the ordinate of design spectrum can be determined as in Section § 3.2.3.2.1 of the NTC (2018) code. The final output takes the form of response spectra in acceleration, relative to each LS, as also reported in Figs. 1a, 1c, and 1e.

In detail, in Eq. 1, V_R denotes the reference life of the structure, which is calculated as the product of the class of use (C_U) and the nominal life (V_N). The latter is defined as the period of time in which the construction remains able to fulfil its original functionality. Finally, P_{VR} is the probability of exceeding the reference period, as indicated in Table 1.

Moreover, from the response spectra in terms of pseudo-acceleration $S_a(T)$ it is possible to pass to the spectra in terms of displacement $S_d(T)$ as follows:

$$S_d(T) = S_a(T)\left(\frac{T}{2\pi}\right)^2 \tag{2}$$

where *T* is the natural period of the SDOF system, or equivalently its natural frequency is given by $\omega = 2\pi/T$. Examples are reported in Figs. 1b, 1d, and 1f.

Table 1 - P_{VR} and T_R variation for the considered LS, in accordance with NTC (2018).

Limit State		P_{VR} **[%]**	T_R **[years]**
Serviceability LS	OLS	81	30
	DLS	63	50
Ultimate LS	SLS	10	475
	CLS	5	975

For the comparative calculations carried out in the present study for selected structural systems made of glass, the return time for a nominal life V_N= 50 years and class of use II (C_u = 1) is calculated for the reference LSs, as shown in Table 1. According to NTC (2018) and based on the grid built on the national territory, for each LS and reference site the seismic hazard is assessed as a function of a_g; design ground acceleration on rigid (rock or rock-like formation) and horizontal soil; F_0, maximum value of spectrum amplification factor; and T_C*, start period of the branch at constant speed of the spectrum in horizontal direction. Local sites characterised

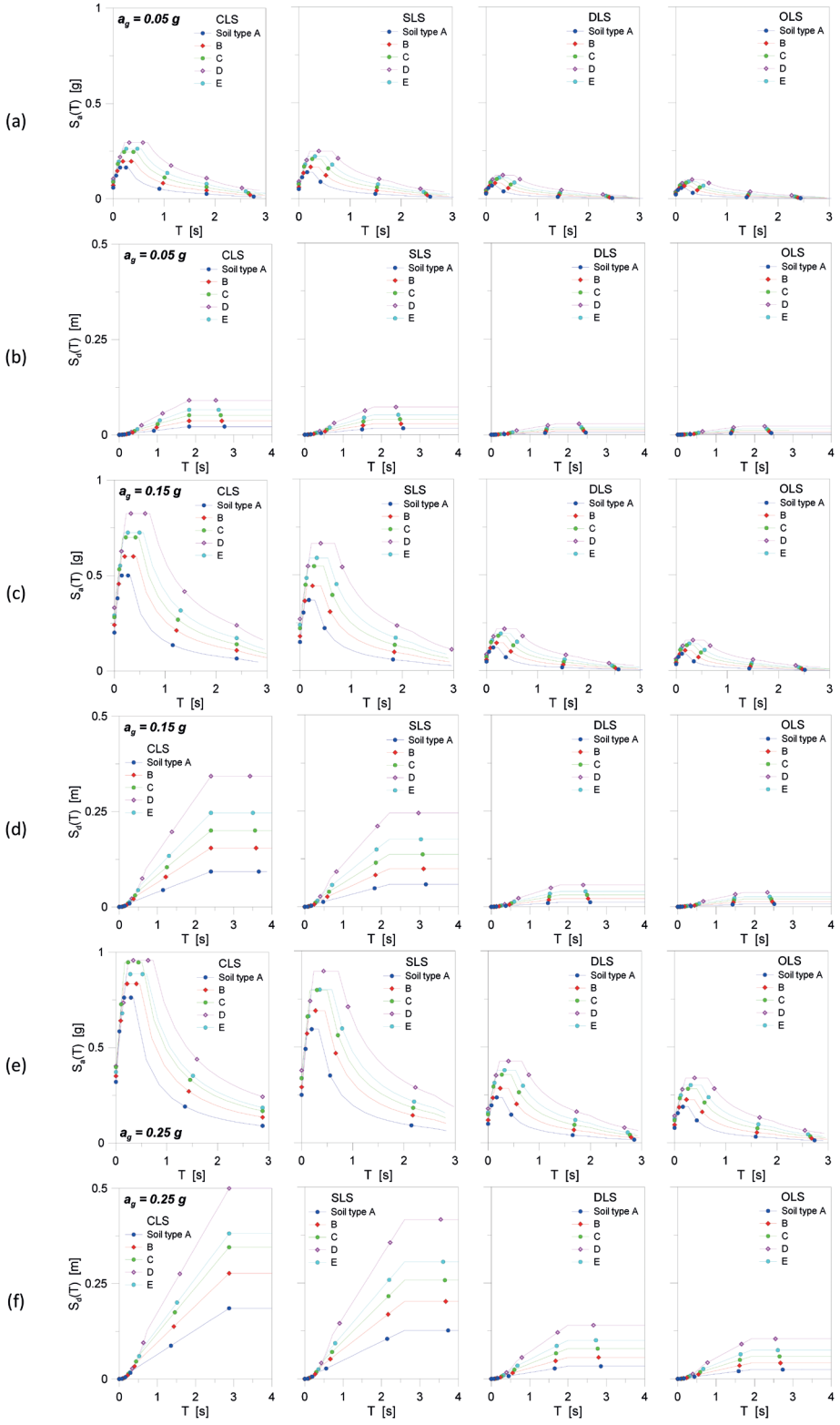

Fig. 1 - Design spectra characterised by different a_g parameters corresponding to soil types A to E and LS performance level in acceleration: a) a_g = 0.05 g, c) a_g = 0.15 g, e) a_g = 0.25 g; or displacement: b) a_g = 0.05 g, d) a_g = 0.15 g, f) a_g = 0.25 g.

by different seismic hazard are thus considered in function of the Italian seismic classification, whereby the national territory is divided.

Since 2003, with the Ordinance of the President of the Council of Ministers n. 3274 (OPCM, 2003), the seismic classification of territory has undergone changes, leading to the introduction of Zone 4 and the concept of probability of occurrence of a seismic event with maximum acceleration peak on rigid soil. In 2006 (OPCM, 2006), acceleration intervals were introduced with 10% probability of exceedance in 50 years, to be attributed to the four seismic zones. Today, the seismic classification remains a useful tool for planning management and for territory control by competent authorities. From a design point of view, however, this has been replaced in the regulatory code by a specific evaluation to carry out based on geographical coordinates of the site and the nominal life of building. Thus, in the present study, the suggested maximum values as in Table 2 are taken as a reference for parametric calculations in zones 1, 2, and 3, respectively.

Table 2 - Conventional maximum horizontal anchor acceleration for the elastic response spectrum.

Seismic zone	a_g
1	0.35 g
2	0.25 g
3	0.15 g
4	0.05 g

3.2. Simplified method proposed by CNR-DT210 guideline for expeditious practical applications

Under basic approximations, it is recognised that for very small *T* values (i.e. as it is for very rigid structures) and for very large *T* values (i.e. highly deformable structures), the accelerations or displacements of a simple oscillator tend to coincide with the corresponding quantities of ground motion. Moreover, the typical trend of pseudo-displacement shows that, for *T* greater than T_D, the fourth constant branch relative to the maximum displacement value is reached.

The streamlined method at Annex § 4.11 of CNR-DT210 (2013) document (Table § 4.19), in this context, consists in assuming the value corresponding to the threshold at CLS as maximum displacement at the site, which is then scaled with different coefficients (1 <) for the other LSs of interest. The so-defined 'multiplicative factors' of seismic demand are thus provided in Annex § 4.11 for design, as also reported in Table 3, and also recommended by FEMA (1997).

Table 3 - Summary of reference 'multiplicative factors' recommended in Annex § 4.11 of CNR-DT210 (2013) document for preliminary seismic demand assessment.

Limit State	Maximum ground displacement normalised to CLS ($d_{max}/d_{max,CLS}$)	Maximum ground displacement normalised to CLS (FEMA273) ($d_{max}/d_{max,CLS}$)
OLS	0.085	0.08
DLS	0.22	0.20
SLS	0.71	0.60
CLS	1	1

To summarise, an overall cautionary estimation of the expected drift demand is carried out based on the use of response spectra in terms of displacement, which provide the maximum values of oscillator response with good approximation. The maximum displacement of a given Multi-Degree of Freedom (MDOF) structure as in Fig. 2 is, hence, achieved by recalling the typical triangular shape of its first mode deformation. To this end, it is assumed that the maximum ground displacement ($d_{max,G}$) is related to the maximum displacement at the top of the frame ($d_{max,MDOF}$) as:

$$d_{max,MDOF} = \Gamma d_{max,G} \tag{3}$$

where the coefficient Γ, defined as the modal participation factor for the first linear modal shape, for structures whose masses are uniformly distributed over the height can be approximated by the following expression [§ C.7.2.10, NTC (2018)]:

$$\Gamma = \frac{3n}{(2n+1)} \tag{4}$$

with *n* representing the number of floors. The required inter-story drift is thus given by:

$$D_p = d_{max,MDOF}/n \tag{5}$$

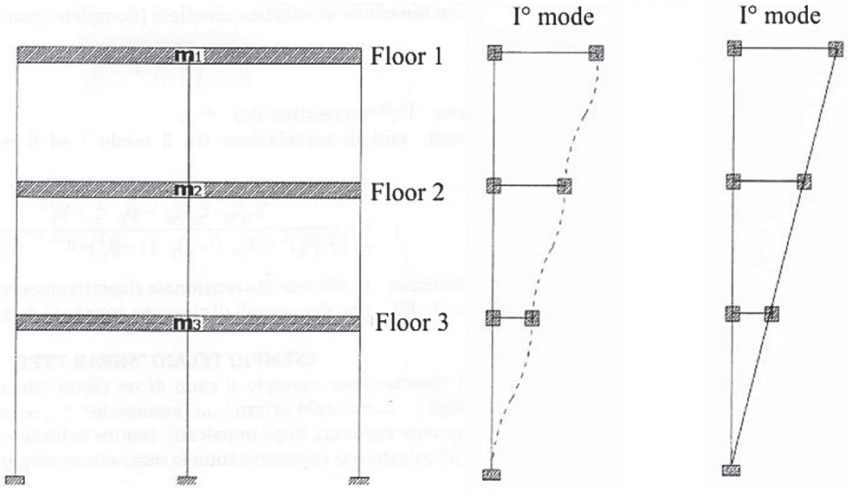

Fig. 2 - MDOF frame and triangular approximation of its first modal shape.

In the present study, the so-called multiplicative factors are preliminary calculated based on Eq. 6 for different cases of examined seismic action, in order to compare the so-derived parametric numerical output with the recommended values listed in Table 3 (CNR-DT210, 2013), where:

Multiplicative Factor = d_{LS_i}/d_{CLS}. (6)

In Eq. 6, d_{LSi} and d_{CLS} represent the maximum displacement demand corresponding to the *i*-th LS under investigation (namely OLS, DLS, or SLS from Table 3) and the most severe CLS, respectively.

Typical results from Eq. 6 are reported in Fig. 3, where the legend of normalised plots assumes, for sake of clarity, that $d_{max,MDOF} = d$ in each examined LS. To facilitate the readability of comparisons, moreover, charts are grouped, from the left to the right, in terms of specific *i*-th LS (OLS, DLS, and SLS, respectively) and, from top to bottom, in terms of chosen seismic zone. Variations in plots are, then, represented by used soil type for the analysis (A to E).

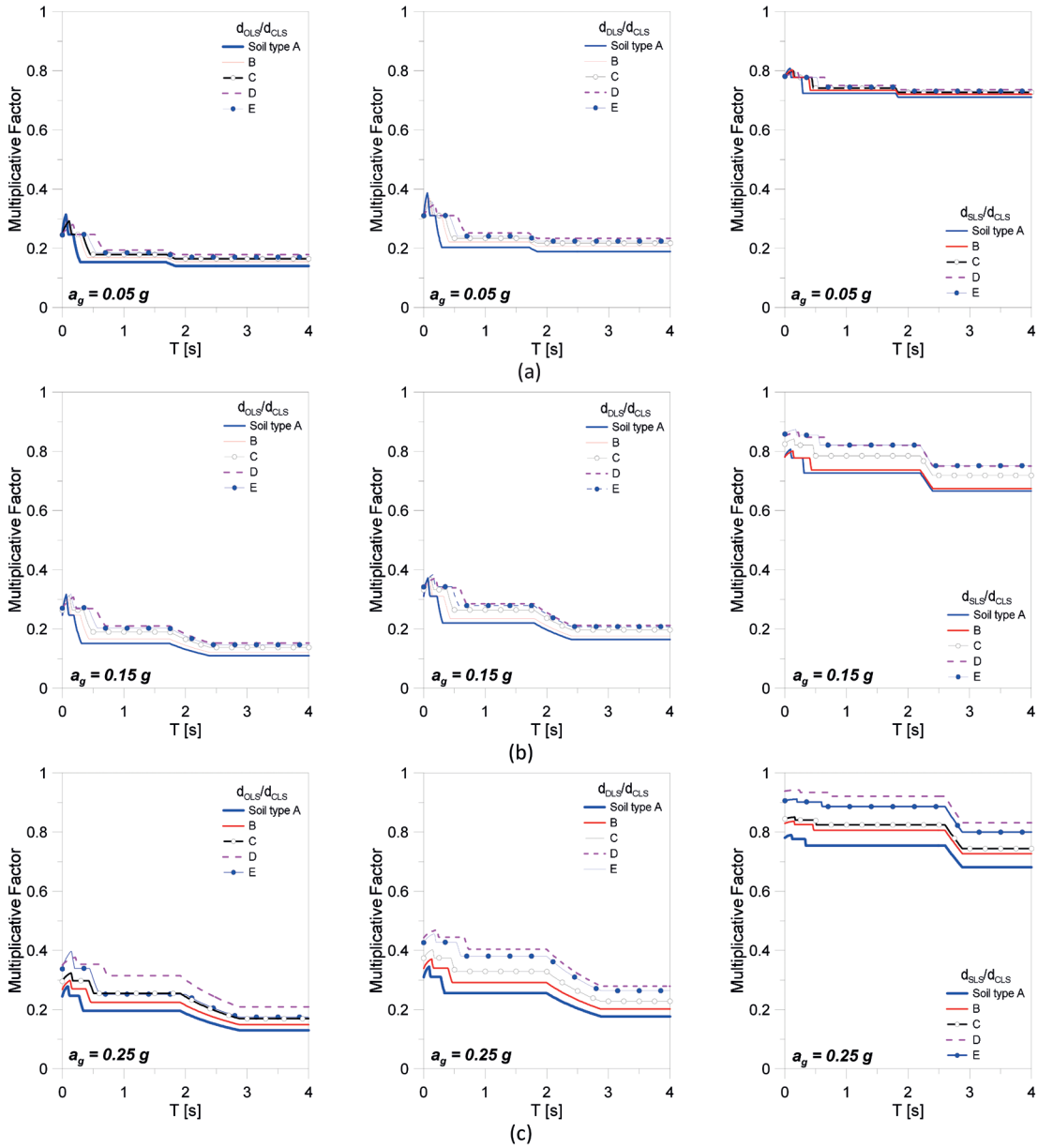

Fig. 3 - Trend of derived 'multiplicative factors' of seismic demand, calculated as $S_d(T)/S_{d\_CLS}(T)$, for the three chosen seismic zones: a) a_g = 0.05 g, b) a_g = 0.15 g, and c) a_g = 0.25 g.

From the proposed comparative output, an almost constant trend of parametric numerical curves with *T* can be noted, for each soil type and seismicity level. This trend, however, tends to a greater variability as the seismicity increases (a_g = 0.05 to 0.25 g), and also with changes in soil type (A to E). The standard deviation of numerical plots, more in detail, can be calculated at around 1-2% for low seismicity (a_g = 0.05 g), 2-4% for medium seismicity (a_g = 0.15 g) and 3-6% for high seismicity (a_g = 0.25 g), as can also be noted in the last column of Table 4. In summary, the parametric analysis confirms that the use of multiplicative factors as in Table 3 allows to rapidly estimate the inter-story drift demand for preliminary design of a given system, based on the site where the building is located, the type of soil, and the considered LS. The presently calculated factors in Fig. 3 and Table 4 are in fact very similar to those in Table 3, for most of the examined configurations. The exception is represented by OLS, where the calculated average scatter is higher than at least 50%, compared to Table 3, and could thus suggest the presence of overconservative design assumptions.

Table 4 - Values of $S_d(T)/_{Sd\_CLS}(T)$ ratio corresponding to the constant branch of spectral displacement ($T > T_D$).

Limit State	Soil type A	Soil type B	Soil type C	Soil type D	Soil type E	σ (%)
OLS_a_g=0.05 g	0.14	0.15	0.16	0.18	0.17	±1.5
DLS_a_g=0.05 g	0.19	0.21	0.22	0.23	0.22	±1.7
SLS_a_g=0.05 g	0.71	0.72	0.73	0.74	0.73	±1.0
CLS_a_g=0.05 g	1.00	1.00	1.00	1.00	1.00	-
OLS_a_g=0.15 g	0.11	0.12	0.14	0.15	0.15	±1.8
DLS_a_g=0.15 g	0.16	0.18	0.20	0.21	0.21	±2.1
SLS_a_g=0.15 g	0.67	0.67	0.72	0.75	0.75	±4.1
CLS_a_g=0.15 g	1.00	1.00	1.00	1.00	1.00	-
OLS_a_g=0.25 g	0.13	0.15	0.17	0.21	0.17	±3.0
DLS_a_g=0.25 g	0.18	0.20	0.23	0.28	0.26	±4.2
SLS_a_g=0.25 g	0.68	0.73	0.74	0.83	0.80	±5.9
CLS_a_g=0.25 g	1.00	1.00	1.00	1.00	1.00	-

3.3. Fragility curves

In recent years, the critical role of glass elements in the assessment of expected losses has been underlined both by observed damage after earthquakes and by several studies. In order to properly define the probability of damage of structural and non-structural components, for each examined LS, it is necessary to know the seismic fragility of components. Fragility curves are known to represent the tool through which the structural vulnerability of buildings (and components) can be efficiently assessed. Namely, seismic vulnerability is the propensity of a structure to be damaged due to a seismic event with a given intensity. Therefore, the vulnerability concerns the seismic action and the damage caused to the physical system. In particular the fragility, in a probabilistic sense, expresses the probability of exceeding a predetermined LS for a predetermined seismic intensity as:

$$F_i(EDP) = \Phi\left(\frac{\ln\left(\frac{EDP_i}{\theta}\right)}{\beta}\right) \quad (7)$$

where F_i denotes the *EDP*-based fragility curve, Φ is the standard normal cumulative distribution function, θ and β are the mean value and the logarithmic standard deviation, respectively, of response parameter, which is termed 'engineering demand parameter' (*EDP*).

In this study, the first statistical moment directly corresponds to a certain damage state threshold related to the violation of some limit state. Moreover, uncertainties are estimated by a linear regression approach on a cloud of data pairs (input-*IM*, output-*EDP*) derived by running a series of dynamic FE numerical simulations. Usually, the first-mode spectral acceleration [$S_a(T_1)$] is considered as a measure of seismic intensity, whereas the drift (*IDR*) is assumed as *EDP*, which is well-related to performance levels. One major advantage of the cloud method is that the coefficients are accurate across the full range of intensities covered by the utilised seismic intensity values.

Of fundamental importance in addressing the construction of fragility curves is the identification of damage thresholds. This can be achieved by various approaches, which are often not directly related to each other, such as code prescriptions or empirical evidences (Mattei and Bedon, 2021).

In this study, a quantitative measure to assess the accuracy and overestimations from the application of the simplified method from the CNR-DT210 (2013) guideline is carried out on fragility curves, which are used to characterise the seismic response of case-study systems CS#1 and CS#2. Such a comparative evaluation is of major concern because the simplified method recalled in section 3.2 does not take into account the specific mechanical and geometrical features of a given system (and, thus, possible local and global criticalities for collapse prevention) but only the maximum required demand (which is related to the site of interest and based on the definition of the response spectrum by seismic codes). On the contrary, the reported fragility curves are developed from refined FE numerical, non-linear dynamic analysis of selected systems CS#1 and CS#2, and are, thus, inclusive of material constitutive behaviours, structural details, and local phenomena.

4. Numerical analysis and discussion of comparative results

Two separate applications of seismic demand assessment methods are presented for different typologies of glass systems. First, the simplified method for the assessment of required displacement capacity by means the synthetic representation of seismic loads as in CNR-DT210 (2013) is examined. Successively, considerations based on the outcomes of vulnerability assessment method through fragility estimation are presented. The aim of such a kind of quantitative comparison is to assess the overestimation error expected from a roughly simplified (but rather efficient for design practice) model with respect to a more detailed FE numerical approach, which allows to consider the majority of mechanisms embodied in the structural dynamic response of glass assemblies.

4.1. Selected systems: features and modelling

The two selected case-study systems, as also previously explored in Mattei and Bedon (2021), are considered in this study in terms of geometrical and mechanical parameters, and further analysed. More in detail, CS#1 detects a glass frame with base steel connections, characterised by a natural period $T_{1,CS\#1}$ = 0.3 s, while CS#2 represents a two-sided adhesively restrained glass panel with a period of vibration $T_{1,CS\#2}$ = 0.65 s, see Fig. 4.

In the former, CS#1, the span is about 8 m long with columns 6 m high. The connections were designed in order to obtain an ideal pinned restraint at the beam-to-column intersection, while the base restraints were characterised by the use of bolted connections and mild steel brackets fixed to the foundation. The second case-study, CS#2, represents a classical non-structural glass component of typical use in buildings, namely a single glass wall spanning between inter-storey floors with a nominal height of 3.5 m and a total width of 1 m.

The FE computational tool required broadening and deepening the modelling of the mechanisms triggered when such systems are subjected to horizontal in-plane actions, giving importance in the numerical model to the glass material and details of the connections. More in detail, regarding the mechanical characterisation of glass for damage detection, a concrete damaged plasticity (CDP) law was used for CS#1 and an infinitely elastic law was chosen for CS#2 [see also Mattei and Bedon (2021)]. In the former case, the input parameters were derived by several authors who calibrated the CDP model to catch the structural brittleness of glass material in typical building applications (Santarsiero *et al.*, 2018; Bedon *et al.*, 2019b). In the latter case, the elastic constitutive law was preferred to allow reducing the computational effort of non-linear dynamic analyses, by monitoring the tensile stress evolution in glass elements and by considering the damage state reached at the first exceedance of material strength value.

In both CS#1 and CS#2 cases, nominal material parameters for glass were taken into account, such as a modulus of elasticity (E_g) of 70 GPa, a Poisson ratio (v_g) equal to 0.23 and a characteristic tensile strength (σ_{tk}) up to 70 MPa.

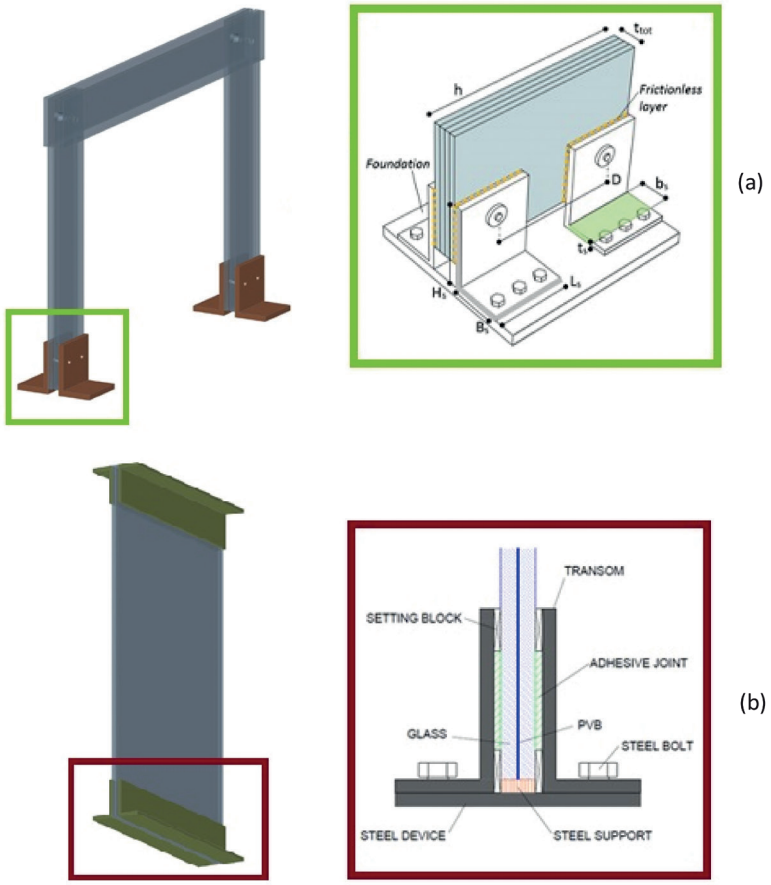

Fig. 4 - Schematic representation of geometrical layout and connection details for the examined case-study systems: a) CS#1, b) CS#2.

Most importantly, the presented CS#1 and CS#2 examples confirm the use of specific mechanical characterisation of glass for damage detection and load-bearing capacity assessment, which, as in the present study, can be reasonably calibrated case by case. In CS#2, the 'ultimate condition' for the shear wall system is assumed to coincide with the first fracture of glass, given that the double laminated glass section is not able to offer any kind of residual load-bearing capacity after partial fracture. In this sense, the use of damage mechanical laws for glass would have no technical utility for simulations and comparative analyses. On the other side, a similar assumption for the CS#2 system, characterised by four glass layers in the thickness of resisting cross-sections, would unavoidably and severely underestimate the real load-bearing capacity of the system, even under partial / limited glass fracture.

4.2. Analysis based on a simplified method

Both CS#1 and CS#2 assemblies can be assimilated to SDOF systems. As such, since the maximum displacements foreseen by the CNR-DT210 (2013) guidelines are known for each LS and type of soil, the rates of spectral displacement, with the maximum value that leads to structural collapse, can be rapidly calculated. In this study, the latter was obtained for CS#1 and CS#2 by means of non-linear dynamic analysis performed in ABAQUS/Explicit (Simulia, 2022), based on the application of 60 natural and unscaled accelerograms, once determined the collapse condition corresponding to the displacement of the first observed crisis, whether glass

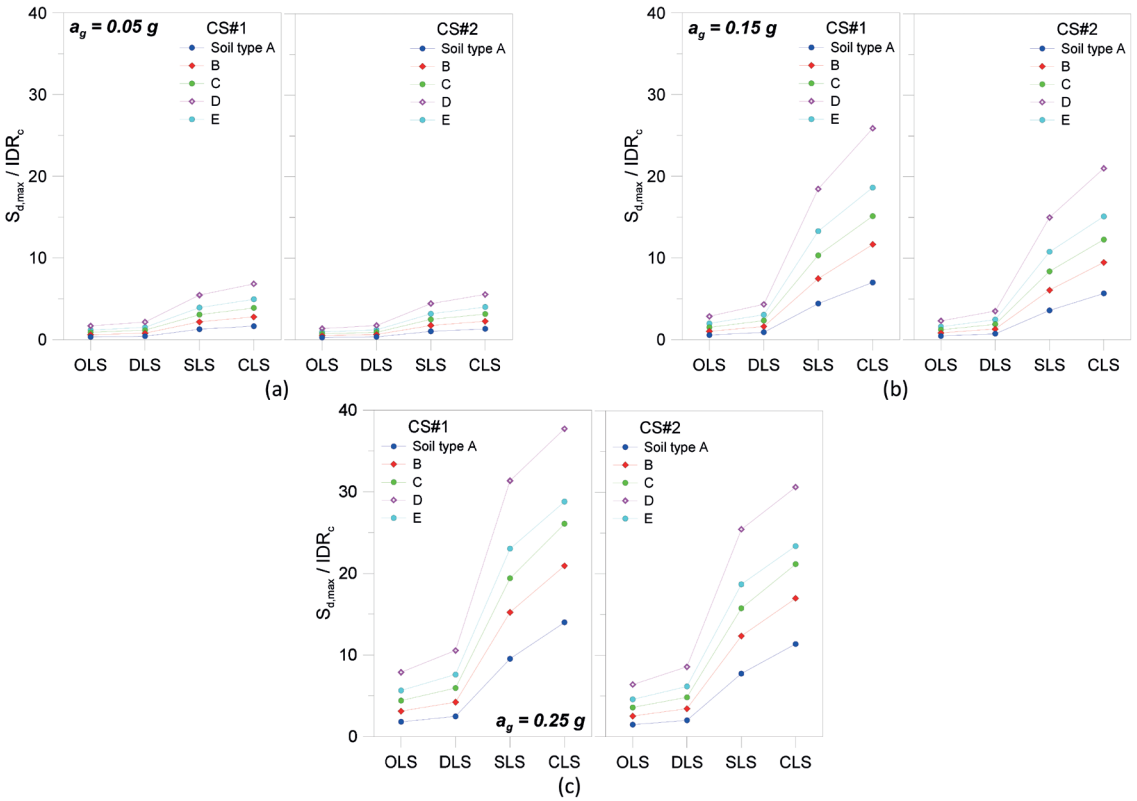

Fig. 5 - Analysis of the ratio of maximum spectral displacement, $S_{d,max}$, to inter-story drift from FE numerical analysis, IDR_c, with respect to the LS and considering three seismic zones: a) a_g = 0.05 g, b) a_g = 0.15 g, and c) a_g = 0.25 g.

cracking or any other failure mechanism of other assembly components (Mattei and Bedon, 2021; Mattei *et al.*, 2021). Two reference displacements are thus taken into account for inter-story drift analysis (*IDR*) and related to the maximum values obtained by FE analysis in seismic conditions, namely $IDR_{c,1}$ = 0.13 m and $IDR_{c,2}$ = 0.16 m for CS#1 and CS#2, respectively (Mattei and Bedon, 2021).

The so-calculated $S_{d,max}/IDR_c$ ratios are proposed in Fig. 5 for every possible combination of soil type, LS and seismicity, grouped by examined system (CS#1 and CS#2, respectively). From Fig. 5 it is clear that for both CS#1 and CS#2 the simplified method in CNR-DT210 (2013) tends to overestimate the expected seismic response, and, therefore, provides much greater results than refined FE numerical analyses. The simplified method from the CNR-DT210 (2013) guideline, in fact, typically refers to flexible structures, i.e. characterised by very low stiffness (and, thus, very high natural period *T*), while it could suffer from overconservative estimations in the case of systems with low *T* value.

Moreover, as an additional check, the $S_d(T_1)/IDR_c$ ratios are also shown in Fig. 6 with reference to the actual period of CS#1 and CS#2 systems. The reported values still show that the simplified calculation method provides largely conservative estimates for the examined assemblies. For example, given that according to the current regulatory codes glass elements are considered as secondary and, therefore, designed to limit or avoid any damage, the DLS is assumed as a reference. For the CS#1 system, in the case of soil B or even C (as it is commonly in the Italian

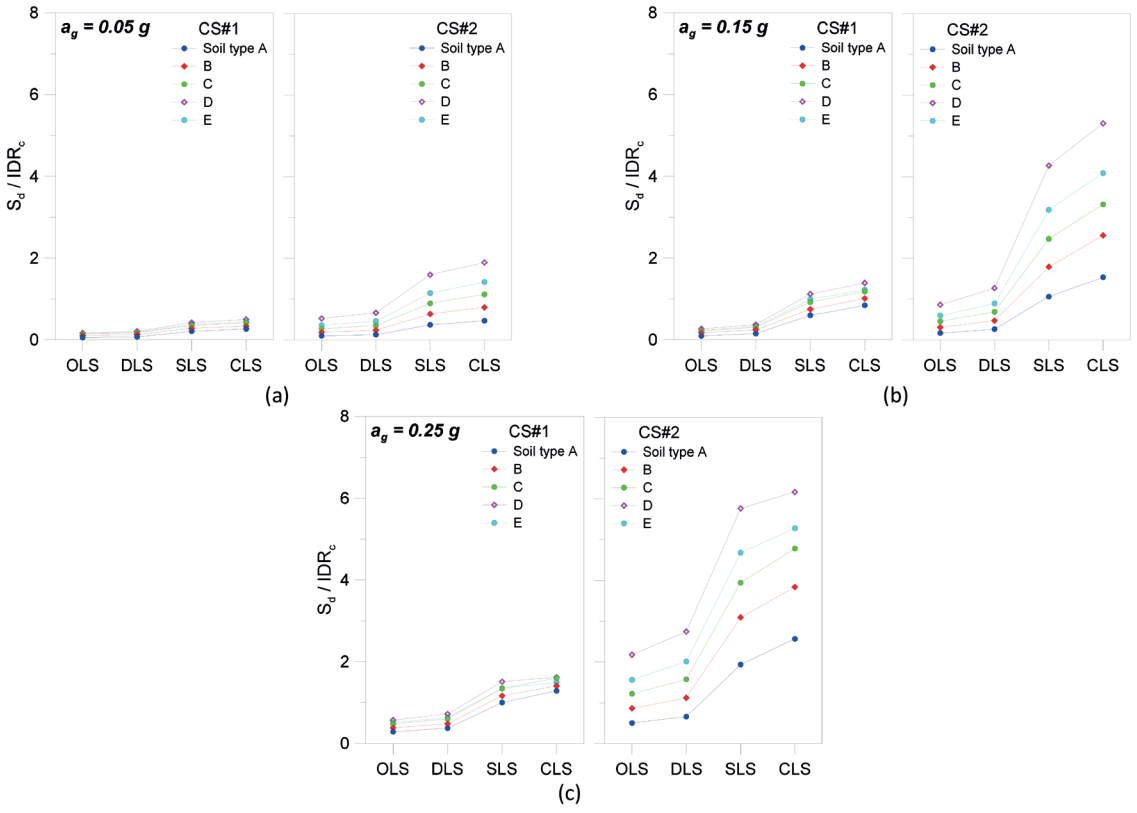

Fig. 6 - Analysis of the ratio of spectral displacement related to the natural period, $S_d(T_1)$, to inter-story drift from FE numerical analysis, IDR_c, with respect to the LS and considering three seismic zones: a) a_g = 0.05 g, b) a_g = 0.15 g, and c) a_g = 0.25 g.

territory), spectral displacements equal to the 13 and 17% part of those obtained from more refined FE numerical analysis can be noted, for B and C soil, respectively. Very similar results are obtained for the CS#1 system under various conditions, with a typical shape of the curves tending to settle at an average of 1. On the contrary, considering in Eq. 2 the spectral displacement corresponding to T_1 for CS#2, much higher ratios (and rather far from 1) are detected in Fig. 6.

4.3 Analysis based on fragility curves

Finally, the EDP-based fragility curves, as obtained in a previous work (Mattei and Bedon, 2021; Mattei *et al*., 2021) by the Cloud Method, are used in this study to assess the extent of over-sizing in terms of probability of over-damage, since it is already known that the thresholds are exceeded. In particular, the Cloud Analysis has been employed in Mattei and Bedon (2021) and Mattei *et al.* (2021) due to its simplicity and using a large suite of records (Bakalis and Vamvatsikos, 2018; Ghosh and Chakraborty, 2020). The imposed set of 60 natural acceleration-time histories, from different magnitudes (i.e. CS#1: M = 4.3-7.6; CS#2: M = 3.9-6.9) and closest distance to the fault rupture (i.e. CS#1: R = 4-63 km; CS#2: R = 1.5-64 km), was chosen from the European Strong Motion Database (https://www.irsn.fr/EN/Research/Scientific-tools/Databases/Pages/European-Strong-Motion-Database-876.aspx) to ensure that a wide range of structural response, until collapse, has been included. The selected records present peak ground acceleration (*PGA*) which ranges in absolute value, for CS#1, between 0.61 and 8.51 m/s^2, and between 0.71 and 8.51 m/s^2, for CS#2. Instead, the spectral acceleration corresponding to the fundamental period, T_1, for CS#1 and CS#2 ranges between 1.05 and 18.63 m/s^2, and between 0.08 and 10.31 m/s^2, respectively. The elastic spectra for the two separate sets are summarised in Fig. 7.

The non-linear dynamic analyses have been performed in ABAQUS/Explicit (Simulia, 2022) and the two probabilistic parameters (ϑ, β) have been obtained by linear regression analyses in logarithmic space for a coherent range of intensity measures, with regard to the drift thresholds for a specific damage state (see Mattei and Bedon, 2021). Two *IDR*, representing two different damage levels, were chosen for CS#1, namely 'Collapse A' and 'B', relative to achieving the maximum tensile stress in glass (i.e. collapse) without or with the ductile contribution of

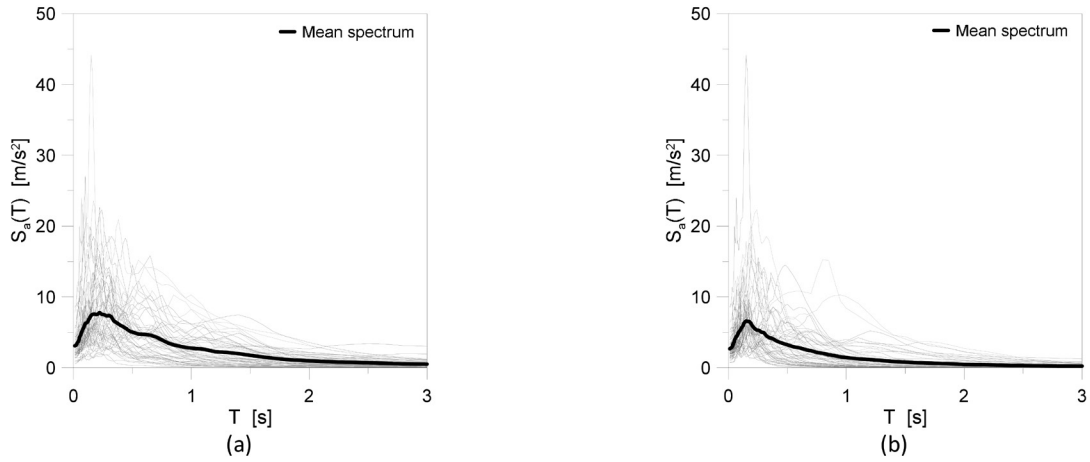

Fig. 7 - Acceleration response spectra (light lines) and mean response spectrum (heavy line) for the accelerograms under consideration for CS#1 (a) and CS#2 (b).

steel base connection (Fig. 4a). For CS#2, the in-plane horizontal relative displacements were considered, corresponding to glass fall-out according to international technical codes that directly or indirectly deal with seismic design of glassed curtain walls [NTC (2018), EC8 (1998), ASCE7-10 (2013), and JASS14 (1996)]. The so-derived EDP-based fragility curves are reported in Fig. 8 for CS#1 and CS#2 assemblies.

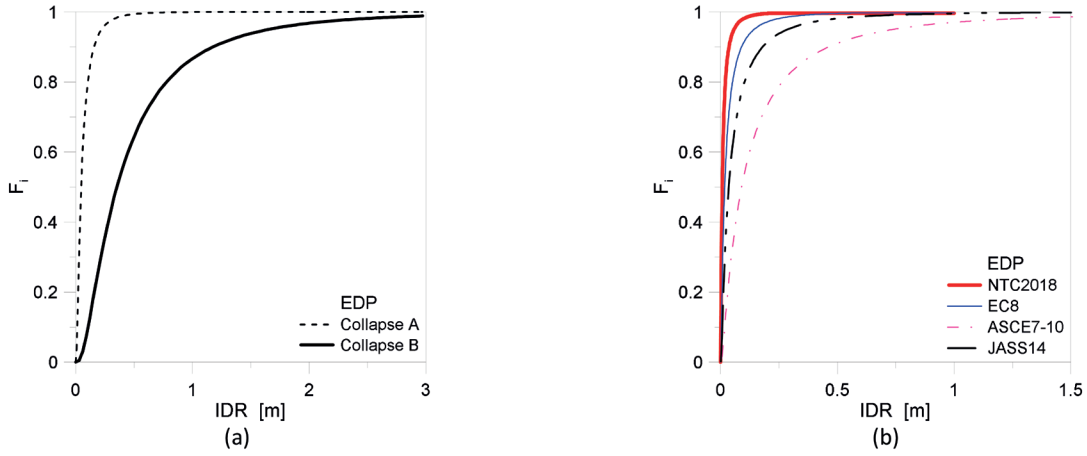

Fig. 8 - EDP-based fragility curves for CS#1 (a) and CS#2 (b).

In Fig. 9, the probability of achieving the threshold by intersection of the EDP-based fragility curves (from Fig. 8a), and the maximum spectral displacement ($S_{d,max}$) is shown for CS#1 assembly in panels a, c, and e.

It is worth noting that, choosing DLS as the performance level for which the system will be built, and considering in a conservative way the 'Collapse A', that takes into account the brittle breakage of glass (i.e. rigid base restraint, without ductile steel bracket as in Fig. 4a), the calculated probability always exceeds 85%, unless a rock soil is considered. This means that, even in the case of low-intensity seismic events, it is very likely that the obtained relative displacement will be higher than the displacement for which the CS#1 system is considered to collapse. However, a more realistic behaviour of the CS#1 assembly is embodied in the discussion of 'Collapse B' results, where the base connection system as in Fig. 4a is taken into account for FE non-linear dynamic analyses. It can thus be noted that the use of the simplified calculation method from CNR-DT210 (2013) document would not be prudent at all. Concerning the results relative to the spectral displacement $S_d(T_1)$ in Fig. 9 for CS#1 (i.e. panels b, d, and f), it can be seen that percentage values close to zero are obtained. This means that the application of the preliminary sizing approach from CNR-DT210 (2013) based on the maximum seismic demand by response spectra is largely restrictive.

In terms of CS#2 assembly performance, Fig. 10 was conceived as for CS#1. Comparative results are, hence, shown by computing the probability of exceedance for $IDR = S_{d,max}$ related to three selected a_g values (0.05, 0.15, and 0.25 g), as well as by real spectral displacement, $S_d(T_1)$, corresponding to the natural period of the examined CS#2 system.

In detail, graphs in panels a-b, c-d, and e-f are grouped, whatever the LS, in terms of fragility curve output representing the various thresholds by selected design codes. As shown, the estimated probabilities of exceedance are highly variable for CS#2. Moreover, in most cases,

the simplified method by the CNR-DT210 (2013) guideline provides values at least 10% higher than the resulting estimates for the corresponding spectral displacements related to CS#2, that is to its 1st-mode period. These findings are easy to justify when the common feature of such a brittle material is pointed out, namely its high stiffness. As a result, the fundamental period of vibration of a given structural system is typically very low, or, in any case, mostly different from the beginning of the last spectrum branch, which is selected for the benefit of safety.

From a practical point of view, assuming the reference LS for design (i.e. DLS) and a typical soil type B, some quantitative outcomes can be further derived. With regard to the simplified method (i.e. Figs. 10a, 10c, 10e), the probability of exceedance overcomes approximately 50% in each case, but for EC8 (1998) it ranges from 75% to 100%. Moreover, focusing on NTC (2018), it can be noted that the probability of exceedance of EDP-threshold remains almost over 85%. As can be expected, since the selected standards assume glassed curtain walls and components

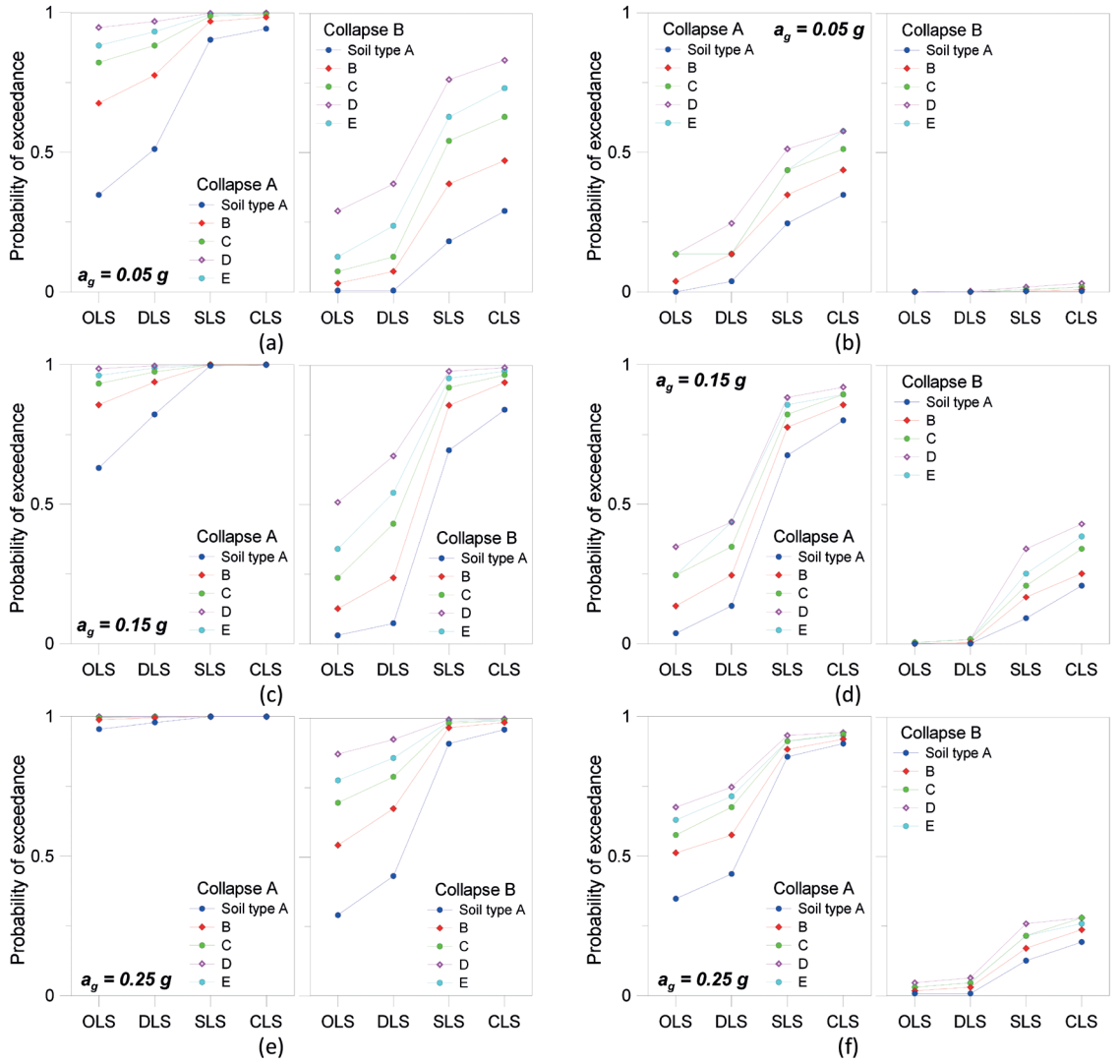

Fig. 9 - Probability of exceedance, for CS#1, of EDP-threshold in correspondence of $S_{d,max}$ for a_g = 0.05 g (a), a_g = 0.15 g (c), a_g = 0.25 g (e); and threshold in correspondence of $S_d(T_1)$ for a_g = 0.05 g (b), a_g = 0.15 g (d), a_g = 0.25 g (f).

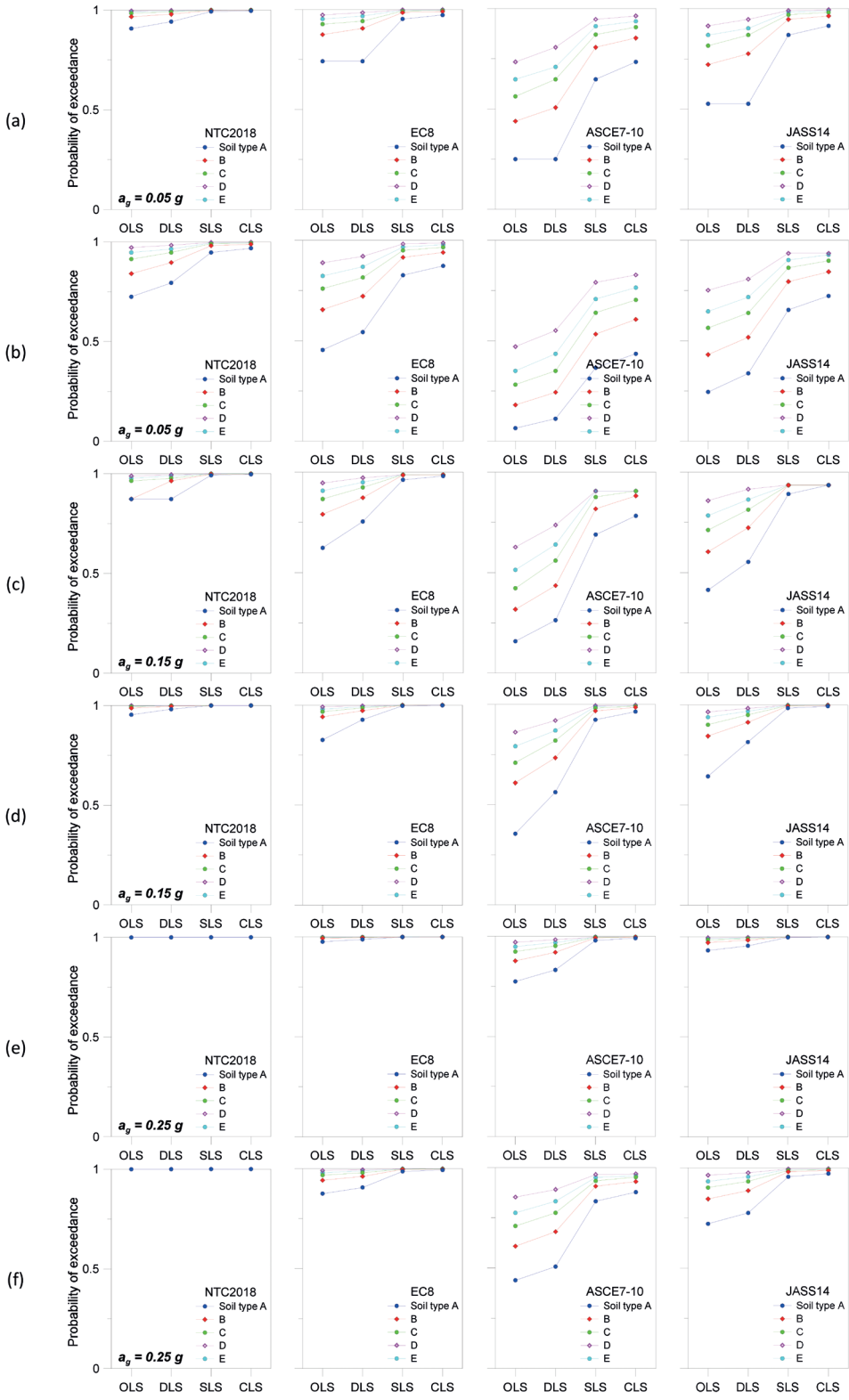

Fig. 10 - Probability of exceedance, for CS#2, of EDP-threshold in correspondence of $S_{d,max}$ for a_g = 0.05 g (a), a_g = 0.15 g (c), a_g = 0.25 g (e); and threshold in correspondence of $S_d(T_1)$ for a_g = 0.05 g (b), a_g = 0.15 g (d), a_g = 0.25 g (f).

as non-structural elements, no specific design criteria or limitations nor appropriate damage parameters can be found in support of design. Otherwise, these codes provide specifications for the type of connection to the primary structure and for the type of material, disregarding the contribution of glass as the building material.

While expanding the discussion of $S_d(T_1)$ results for the CS#2 system (i.e. Figs. 10b, 10d, 10f), in this regard, it is worth noting that the minimum observed values derive from the fragility curve corresponding to EDP-threshold according to ASCE7-10 (2013). The latter provides a specific empirical formulation that can be used (in the absence of full-scale experimental tests) to estimate the maximum inter-storey displacement that a small-size glass panel could accommodate without suffering damage. However, the intrinsic conservative feature of such a simplified calculation is strongly highlighted in Fig. 10 for high seismicity zones (a_g = 0.25 g).

Overall, from the presented comparative results, it is even more evident that the currently available simplified method does not capture at all the seismic response of a given glass construction system and that, especially for the structural design process, does not provide sufficiently accurate results, but necessarily suggests the integrated use of more sophisticated and time-consuming calculation models and simulations (or even full-scale experimental prototypes).

5. Conclusions

Dealing with the seismic design of structural, secondary structural, and non-structural glass systems and components is an issue that has been addressed and widely discussed by the scientific community in recent years. However, several issues and gaps are still open challenges for design. In this regard, the present study has explored in greater detail the accuracy, potentials, and limits of currently available simplified calculation methods compared to more refined but computationally expensive FE numerical models and non-linear dynamic simulations. To this end, basic seismic design principles were first cited and discussed. Specific emphasis was given to the simplified method for the assessment of required capacity in terms of displacement, which is currently suggested for preliminary design by the CNR-DT210 (2013) guideline and based on the definition of design spectra according to the national code NTC (2018). Worthy of note is that the method, even if with specific reference to the Italian code, is in line with design requirements on which current international seismic codes are based. It also provides practical support for rapid design estimates in seismic conditions.

By selecting two different case-study systems made of glass (CS#1 and CS#2) and assimilated to SDOF systems, some considerations were thus presented on the reliability of the CNR-DT210 simplified method. Considerable support was derived from results of extended FE non-linear dynamic analyses performed in ABAQUS/Explicit software (Simulia, 2022) on CS#1 and CS#2 numerical models, intended to accurately capture and explore their seismic behaviour. Moreover, statistical response results represented by structural and non-structural fragility curves were also used to assess the probability of failure in correspondence of maximum inter-story drift by means of spectral displacement calculations. Therefore, the effects of soil classification, performance LS and amplitude of seismic action were taken into account for extensive parametric comparative analyses on CS#1 and CS#2 systems.

Overall, the reported findings confirmed that the use of multiplicative factors in the CNR-DT210 (2013) methodology, such as also recommended by FEMA273 (1997), would typically result in encouraging the wasteful oversizing of building components made of glass, especially for high seismicity zones. In this sense, the support of refined FE numerical models (or even full-

scale experimental prototypes) should in general be preferred, especially to capture local and global damage mechanisms, which are typical of glass assemblies.

Acknowledgments. This research has received no external funding. The study took inspiration from the paper 'Analytical fragility method to assess seismic behaviour of glass panels', by S. Mattei and C. Bedon, that was orally presented during the 39th GNGTS National Conference (Convegno del Gruppo Nazionale per la Geofisica della Terra Solida) and was selected as a recipient of one of the AGLC Licio Cernobori awards for the 2021 edition (topic 'Caratterizzazione sismica del territorio"). In this regard, the AGLC team (Associazione per la Geofisica Licio Cernobori) and the GNGTS scientific committee are gratefully acknowledged.

REFERENCES

Aiello C., Caterino N., Maddaloni G., Bonati A., Franco A. and Occhiuzzi A.; 2018: *Experimental and numerical investigation of cyclic response of a glass curtain wall for seismic performance assessment*. Constr. Build. Mater., 187, 596-609.

ASCE7-10; 2013: *Minimum design loads for buildings and other structures*. American Society of Civil Engineers, Reston, VA, USA, 253 pp.

Bakalis K. and Vamvatsikos D.; 2018: *Seismic fragility functions via nonlinear response history analysis*. J. Struct. Eng., 144, 04018181.

Beason W.L., Meyers G.E. and James R.W.; 1984: *Hurricane related window glass damage in Houston*. J. Struct. Eng., 110, 2843-2857.

Bedon C. and Amadio C.; 2018: *Numerical assessment of vibration control systems for multi-hazard design and mitigation of glass curtain walls*. J. Build. Eng., 15, 1-13.

Bedon C. and Amadio C.; 2019: *ADAS dampers for the hazard protection of multi-storey buildings with glazing envelopes: a feasibility study*. Boll. Geof. Teor., 60, 197-220, doi: 10.4430/bgta0253.

Bedon C., Zhang X., Santos F., Honfi D., Kozłowski M., Arrigoni M., Figuli L. and Lange D.; 2018: *Performance of structural glass facades under extreme loads - Design methods, existing research, current issues and trends*. Constr. Build. Mater., 63, 921-937.

Bedon C., Amadio C. and Noè S.; 2019a: *Safety issues in the seismic design of secondary frameless glass structures*. Saf., 5, 80, doi: 10.3390/safety5040080.

Bedon C., Santarsiero M. and Moupagitsoglou K.; 2019b: *Energy-based considerations for the seismic design of duc-tile and dissipative glass frames*. Soil Dyn. Earthquake Eng., 125, 105710, doi: 10.1016/j.soildyn.2019.105710.

Behr R.A.; 1998: *Seismic performance of architectural glass in mid-rise curtain wall*. J. Archit. Eng., 5, 105-106.

Behr R.A., Minor J.E. and Kremer P.A.; 1996: *Effects of accelerated weathering on architectural laminated glass in a windstorm environment.* In: Proc. Science and Technology of Building Seals, Sealants, Glazing, and Waterproofing Conference, Myers J.C. (ed), ASTM International, Ft. Lauderdale, FL, USA, Vol. 6, 19 pp.

Brueggeman J.L., Behr R.A., Wulfert H., Memari A.M. and Kremer P.A.; 2000: *Dynamic racking performance of an earthquake isolated curtain wall system*. Earth. Spectra, 16, 735-756.

Caterino N., Del Zoppo M., Maddaloni G., Bonati A., Cavanna G. and Occhiuzzi A.; 2017: *Seismic assessment and finite element modelling of glazed curtain walls.* Struct. Eng. Mech., 61, 77-90.

CNR-DT210; 2013: *Istruzioni per la progettazione, l'esecuzione ed il controllo di costruzioni con elementi strutturali di vetro*. Consiglio Nazionale delle Ricerche, Commissione di studio per la predisposizione e l'analisi di norme tecniche relative alle costruzioni, Roma, Italy, 362 pp.

Dean S., Memari A., Chen X., Kremer P. and Behr R.; 2006: *Seismic performance of two-side structural silicone glazing systems*. J. ASTM Int., 3, 100407.

EC8 (Eurocode 8); 1998: Design of structures for earthquake resistance – *Part 1: General rules, seismic actions and rules for buildings.* European Committee for Standardization (CEN), Brussels, Belgium, 229 pp.

FEMA (Federal Emergency Management Agency); 1997: *NEHRP guidelines for the seismic rehabilitation of buildings.* Washington D.C., U.S.A., 426 pp.

Gavanski E.; 2010: *Behaviour of glass plates under wind loads*. Ph.D., University of Western Ontario, Canada, 182 pp.

Ghosh S. and Chakraborty S.; 2020: *Seismic fragility analysis of structures based on Bayesian linear regression demand models.* Probabilistic Eng. Mech., 61, 103081.

Haldimann M.; 2006: *Fracture strength of structural glass elements - Analytical and numerical modelling, testing and design.* Ph.D. Thesis in Environnement Naturel, Architectural et Construit, École Polytechnique Fédérale de Lausanne (EPFL), Lausanne, Switzerland, 222 pp., doi: 10.5075/epfl-thesis-3671.

Haldimann M., Luible A. and Overend M.; 2008: *Structural use of glass*. International Association for Bridge and Structural Engineering IABSE, Zurich, Switzerland, 228 pp., doi: 10.2749/sed010, ISBN 978-3-85748-119-2.

Huang B., Chen S., Lu W. and Mosalam K.M.; 2017: *Seismic demand and experimental evaluation of the nonstructural building curtain wall: a review*. Soil Dyn. Earthquake Eng., 100, 16-33.

JASS14; 1996: *Japanese architectural standard specification curtain wall*. Architectural Institute of Japan, Tokyo, Japan, 349 pp.

Larcher M., Arrigoni M., Bedon C., Van Doormaal J.C.A.M., Haberacker C., Hüsken G., Millon O., Saarenheimo A., Solomos G. and Thamie L.; 2016: *Design of blast-loaded glazing windows and facades: a review of essential requirements towards standardization*. Hindawi Publishing Corporation, Advances in Civil Engineering, Vol. 2016, ID 2604232, 14 pp., doi: 10.1155/2016/2604232.

Mattei S. and Bedon C.; 2021: *Analytical fragility curves for seismic design of glass systems based on cloud analysis*. Symmetry, 13, 1541, doi: 10.3390/sym13081541.

Mattei S., Fasan M. and Bedon C.; 2021: *On the use of cloud analysis for structural glass members under seismic events*. Sustainability, 13, 9291.

Memari A.M., O'Brien W.C., Kremer P.A. and Behr R.A.; 2011: *Architectural glass seismic behavior fragility curve development*. Federal Emergency Management Agency, Washington D.C., USA, Report No. FEMA P-58/BD-3.9.1, 2.

Netusil M. and Eliasova M.; 2012: *Structural design of composite steel-glass elements*. In: Bos F., Louter C., Nijsse R. and Veer F. (eds), Challenging Glass 3, pp. 715-724, doi: 10.3233/978-1-61499-061-1-715.

Niedermaier P.; 2003: *Shear-strength of glass panel elements in combination with timber frame constructions*. In: Proc. 8th International Conference on Architectural and Automotive Glass (GPD), Vitkala J. (ed), Tampere, Finland, pp. 262-264.

NTC (Norme tecniche per le costruzioni): 2018; *Istruzioni per l'applicazione dell'«Aggiornamento delle "Norme tecniche per le costruzioni"» di cui al decreto ministeriale 17 gennaio 2018.* Ministero delle Infrastrutture e dei Trasporti Circolare 21 gennaio 2019, n. 7, C.S.LL.PP, Roma, Italy.

OPCM (Ordinanza del Presidente del Consiglio dei Ministri); 2003: *Ordinanza del Presidente del Consiglio dei Ministri 20 marzo 2003, n. 3274: Primi elementi in materia di criteri generali per la classificazione sismica del territorio nazionale e di normative tecniche per le costruzioni in zona sismica*. G.U. Serie Generale n. 105 del 08-05-2003, Roma, Italy.

OPCM (Ordinanza del Presidente del Consiglio dei Ministri); 2006: *Ordinanza del Presidente del Consiglio dei Ministri 28 aprile 2006, n. 3519: Criteri generali per l'individuazione delle zone sismiche e per la formazione e l'aggiornamento degli elenchi delle medesime zone*. G.U. Serie Generale n. 108 del 11-05-2006, Roma, Italy.

Puga H., Olmos B., Olmos L., Jara J.M. and Jara M.; 2015: *Damage assessment of curtain wall glass*. J. Phys. Conf. Ser., 628, 012052, doi: 10.1088/1742-6596/628/1/012052.

Santarsiero M., Bedon C. and Louter C.; 2018: *Experimental and numerical analysis of thick embedded laminated glass connections.* Compos. Struct., 56, 188-242.

Shelby J.E.; 2020: *Introduction to glass science and technology, 3rd ed*. Royal Society of Chemistry, Cambridge, UK, 341 pp.

Simulia; 2022: *ABAQUS v. 6.14 computer software and online documentation*. Dassault Systems, Providence, RI, USA, 1146 pp.

Sivanerupan S., Wilson J.L., Gad E.F. and Lam N.T.K.; 2014: *Drift performance of point fixed glass façade systems*. Adv. Struct. Eng., 17, 1481-1495.

Tahmasebinia F., Wang Y., Wu S., Ho J., Shen W., Ma H., Sepasgozar S.M.E. and Marroquin F.A.; 2021: *Advanced structural analysis of innovative steel-glass structures with respect to the architectural design*. Build., 11, 208, doi: 10.3390/buildings11050208.

Venkata V.K.; 2004: *Development and testing of hurricane resistant laminated glass fiber reinforced composite window panels*. M.S., University of Missouri, Columbia, MO, USA, 88 pp.

Corresponding author: Chiara Bedon
University of Trieste, Department of Engineering and Architecture
Via Valerio 6/1, 34127 Trieste, Italy
Phone: +39 040 558 3837; e-mail: chiara.bedon@dia.units.it